

Figure 5-15 Cross-sectional views of other strip transmission-line configurations. Their approximate electric field patterns are also shown.

ing complex stripline systems at frequencies as high as 20 GHz. For additional information, the reader is referred to Refs. 5-16, 5-23, and 5-24.

The transmission line pictured in part *b* of Fig. 5-15 is known as *slot line*. It is a useful alternative to microstrip in the fabrication of microwave integrated circuits. For example, since the electric field is as shown, devices can be easily shunt connected to the line. Microstrip, on the other hand, lends itself to series-connected devices. Also, high values of Z_0 are easily realized in slot line, while low values are more easily achieved with microstrip. In slot line, the magnetic field (not shown) has a strong component in the propagation direction. Therefore, the primary transmission mode is *not* TEM but TE. This characteristic is useful when the system requires the incorporation of nonreciprocal ferrite components. The slot line has been analyzed by Cohn (Ref. 5-25) and others (Refs. 5-26 and 5-27). These articles provide detailed design information on velocity, wavelength, and impedance.

The coplanar line, shown in part *c* of the figure, consists of a thin metal strip with ground planes on either side. Also shown is the approximate electric field pattern. This structure has been analyzed by Wen (Ref. 5-28) and Davis (Ref. 5-29). It combines some of the advantages of microstrip and slot lines. For example, both series and shunt connections are easily achieved in coplanar line. Also, since a significant longitudinal magnetic field component is present, nonreciprocal ferrite components can be realized.

An excellent comparison of microstrip, slot line, and coplanar line is found in Ref. 5-7. A wealth of design data is also included.

5-4 RECTANGULAR AND CIRCULAR WAVEGUIDES

Hollow waveguides are commonly used as transmission lines at frequencies above 5 GHz. Compared to coaxial transmission, waveguides have the following advantages.

1. Higher power handling capability.
2. Lower loss per unit length.
3. A simpler, lower cost mechanical structure.

In addition, the reflections caused by the flanges used in connecting waveguide sections is usually less than that associated with coaxial connectors. The disadvantages of waveguide transmission are larger cross-sectional dimensions and a lower usable bandwidth than coaxial transmission. The fact that hollow waveguides can support electromagnetic waves is proven mathematically in Sec. 5-5. The properties of these waves are described in detail and appropriate equations are derived. In this section, the explanation is given in terms of TEM waves and the transmission-line concepts developed in Chapter 3.

5-4a Rectangular Waveguide

Figure 5-16 shows a rectangular waveguide of inner dimensions a and b . This represents the most common configuration for waveguide transmission. It is customary to label the broad dimension or guide width as a and the height as b . Typically, the conducting walls are made of brass or aluminum and the dielectric region is usually air. The following discussion shows that under certain conditions, electromagnetic waves can propagate along the inside of the waveguide. It is assumed that the wall thickness is greater than several skin depths and hence does not enter into the analysis.

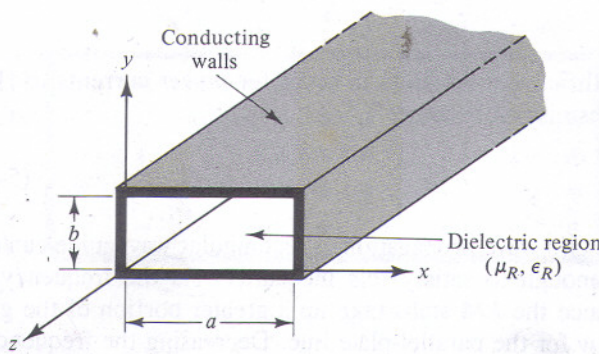


Figure 5-16 The rectangular waveguide structure.

Figure 5-17 shows a parallel-plate transmission line similar to that in Fig. 5-6. The width of the metal strips is w and their spacing is b . The E and H field patterns are also shown. Power is delivered to the load via longitudinal current flow along the two strips. Suppose now that a pair of shorted stubs of length l are connected to the parallel-plate line as shown. If the stubs are a quarter wavelength long, they will have no effect on the transmission of power since they present an infinite impedance in shunt with the line. The E and H standing wave patterns for the shorted stubs are also shown in the figure. The current flow in the stubs is reactive since no real power can be delivered to the shorts. The longitudinal current, on the other hand, can deliver power and hence is referred to as the *power* current. Note that the direction of the *reactive* and *power* currents are perpendicular to each other. One can imagine an infinite set of these quarter wavelength shorted stubs connected in shunt with the parallel-plate line. The resultant configuration is exactly the rectangular waveguide shown in Fig. 5-16 where

$$a = 2l + w$$

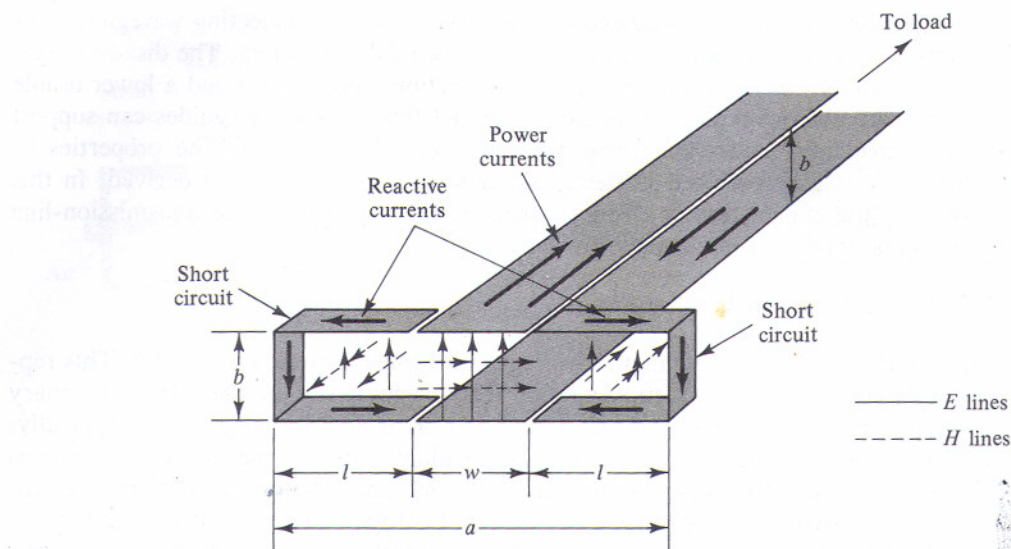


Figure 5-17 The development of rectangular waveguide from a parallel-plate transmission line.

Since $l = \lambda/4$ and the width w must be finite in order for *power* currents to flow, the condition for power transmission becomes

$$a > \frac{\lambda}{2} \quad (5-34)$$

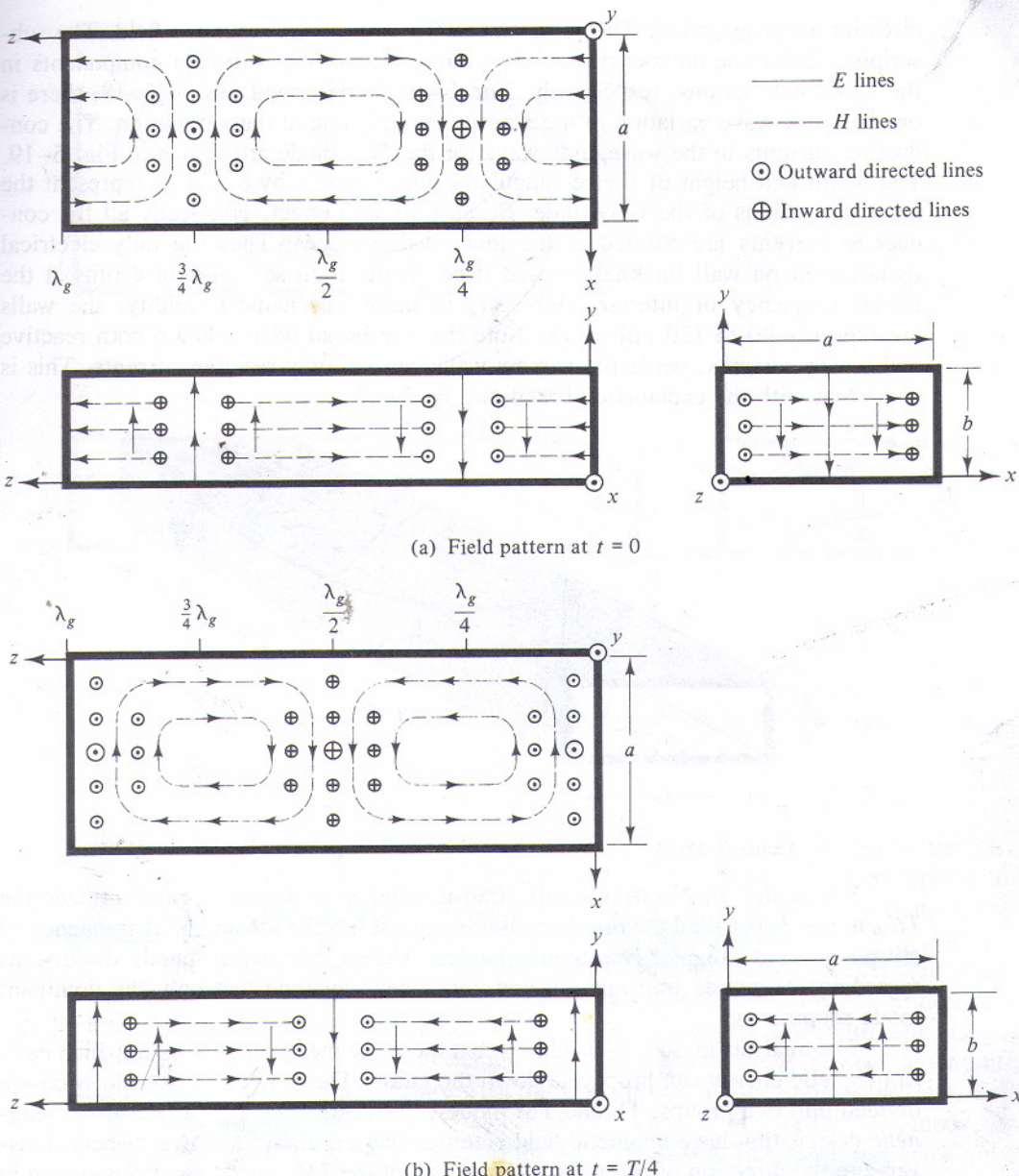
In other words, electromagnetic wave propagation in rectangular waveguide can only occur at frequencies high enough to satisfy this inequality. As the frequency decreases, λ increases and hence the $\lambda/4$ stubs take up a greater portion of the guide width a , leaving less room w for the parallel-plate line. Decreasing the frequency to the point where $a = 2l = \lambda/2$ results in $w = 0$, which prevents the flow of power currents. The frequency at which this occurs is called the *cutoff frequency* (f_c) of the guide. Thus the waveguide has the properties of a highpass filter since power transmission is possible only when $f > f_c$ or $\lambda < \lambda_c$. Using Eq. (5-34), the cutoff wavelength is given by

$$\lambda_c = 2a \quad (5-35)$$

With $f_c\lambda_c = v$, the cutoff frequency of the guide is

$$f_c = \frac{v}{2a} = \frac{c}{2a\sqrt{\mu_R \epsilon_R}} \quad (5-36)$$

What we have described here is the TE_{10} mode of transmission in rectangular guide. Its electric and magnetic field patterns are shown in Fig. 5-18. Based upon the explanation given here, these patterns are plausible. For example, the half sine wave variation of E_y as a function of x can be attributed to the standing waves of the shorted stubs. The fact that the magnetic field is transverse to the direction of propa-

Figure 5-18 The TE_{10} mode pattern as derived from Eq. (5-76).

gation at $x = a/2$ is due to the TEM field pattern of the parallel-plate line. Also, the z component of magnetic field near $x = 0$ and $x = a$ is a consequence of the reactive currents flowing in the shorted stubs. Note that the magnetic lines form complete loops in the x - z plane.

The TE (transverse electric) designation means that for this mode of propagation, the direction of the electric field is always and everywhere transverse to the

direction of propagation. The same *cannot* be said for the magnetic field. The subscripts indicate the number of *half* sine wave variations of the field components in the x and y directions, respectively. For the mode described in Fig. 5-18, there is *one* half sine wave variation in the x direction and none in the y direction. The conduction currents in the waveguide walls for the TE_{10} mode are shown in Fig. 5-19. The width and height of the rectangular guide, denoted by a and b , represent the inner dimensions of the waveguide. Because of skin effect, practically all the conduction currents are located at the inner wall surfaces. Thus the only electrical requirement on wall thickness is that it be greater than several skin depths at the lowest frequency of interest. However, to insure mechanical rigidity, the walls are typically 40 to 120 mils thick. Note that the broad walls contain both reactive and power currents, while the narrow walls contain only reactive currents. This is consistent with the explanation based on Fig. 5-17.

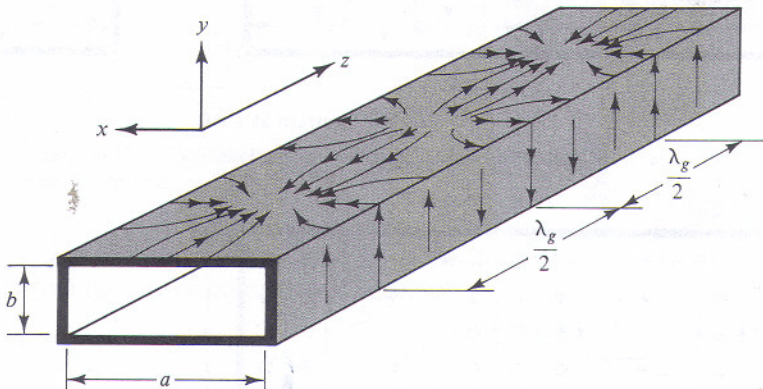
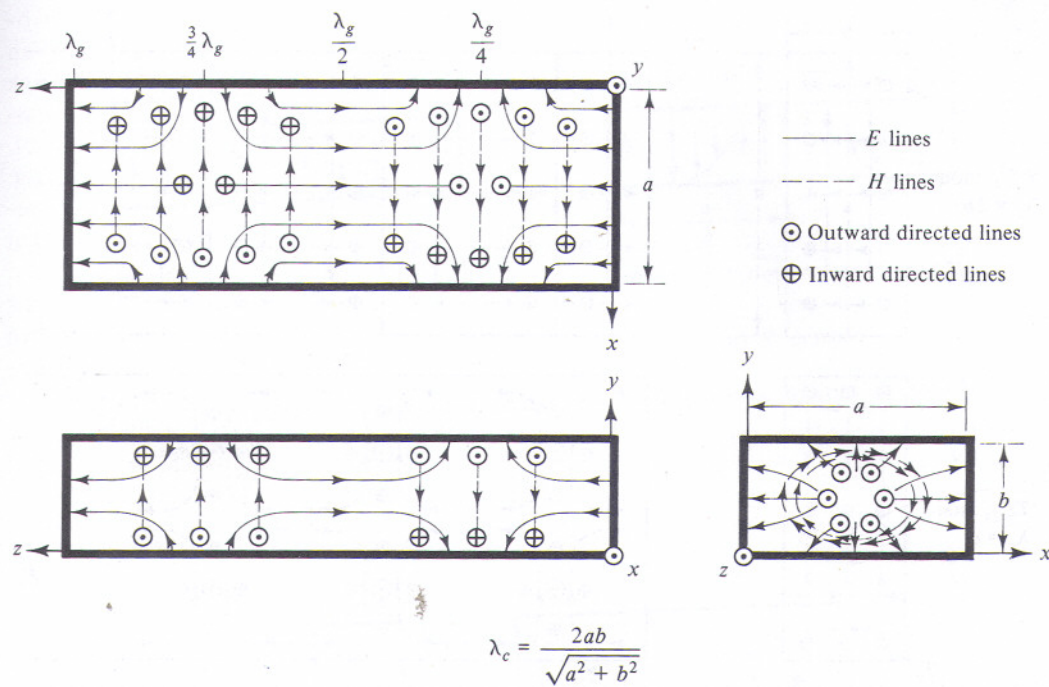


Figure 5-19 Conduction currents in rectangular guide for the TE_{10} mode.

Practically all electromagnetic transmission in rectangular guide utilizes the TE_{10} mode. It is called the *dominant mode* since it has the lowest cutoff frequency of all possible rectangular waveguide modes. Unless otherwise stated, discussions regarding waveguide transmission and components assume that only the dominant mode propagates.

The analysis in Sec. 5-5a shows that there are many other ways in which electromagnetic energy can propagate down the guide. These modes of transmission are divided into two groups, TE and TM modes. Those with the TM or *transverse magnetic* designation have magnetic field patterns that are always and everywhere transverse to the direction of propagation. A sketch of the TM_{11} mode pattern is shown in Fig. 5-20. Its cutoff wavelength is also indicated. The cutoff wavelength and frequency for any mode in rectangular waveguide (whether TE or TM) can be determined from Eqs. (5-67) and (5-68). As stated earlier, the subscripts m and n indicate the number of half sine wave variations of the field components in the x and y directions, respectively.

Sketches of some of the higher-order TE modes with their cutoff wavelengths are shown in Fig. 5-21. Additional TE and TM modes are described in Chapter 5 of Ref. 5-8. The existence of some of these modes can be verified by an argument

Figure 5-20 The field pattern and cutoff wavelength for the TM_{11} mode.

similar to that used for the TE_{10} mode. For instance, the TE_{01} is merely the TE_{10} mode rotated 90° . In this case the b dimension must be wide enough to support the width w and the two quarter wavelength shorted stubs. At cutoff, $w = 0$ and therefore $\lambda_c = 2b$.

The development of the TE_{20} and the TE_{30} modes from a parallel-plate transmission line is indicated in Fig. 5-22. Only the x - y plane is shown. Part a describes the TE_{20} mode in terms of two shorted stubs, one a quarter wavelength long and the other three quarters of a wavelength long. Since both stubs present an infinite impedance, they do not interfere with transmission along the parallel-plate line. Cut-off occurs when $w = 0$ or $a = 0.25\lambda + 0.75\lambda$. Thus $\lambda_c = a$ for the TE_{20} mode. By similar reasoning, one concludes that the TE_{30} cutoff wavelength is $2a/3$ since three half wavelengths must be *squeezed* into the guide width a at cutoff.

Equations for velocity, wavelength, and phase constant in rectangular waveguide have been derived in Sec. 5-5a. The physical argument used thus far is helpful in showing the reasonableness of these equations. Consider the TE_{10} mode as described and developed in Fig. 5-17. It can be thought of as a TEM wave traveling down the waveguide plus two TEM waves propagating in the transverse plane. The conduction currents associated with these waves are shown in Fig. 5-23a, where I_P represents the power currents and I_R the reactive currents. The vector sum of these currents is indicated by two currents (I_T) whose direction of flow is at an angle θ

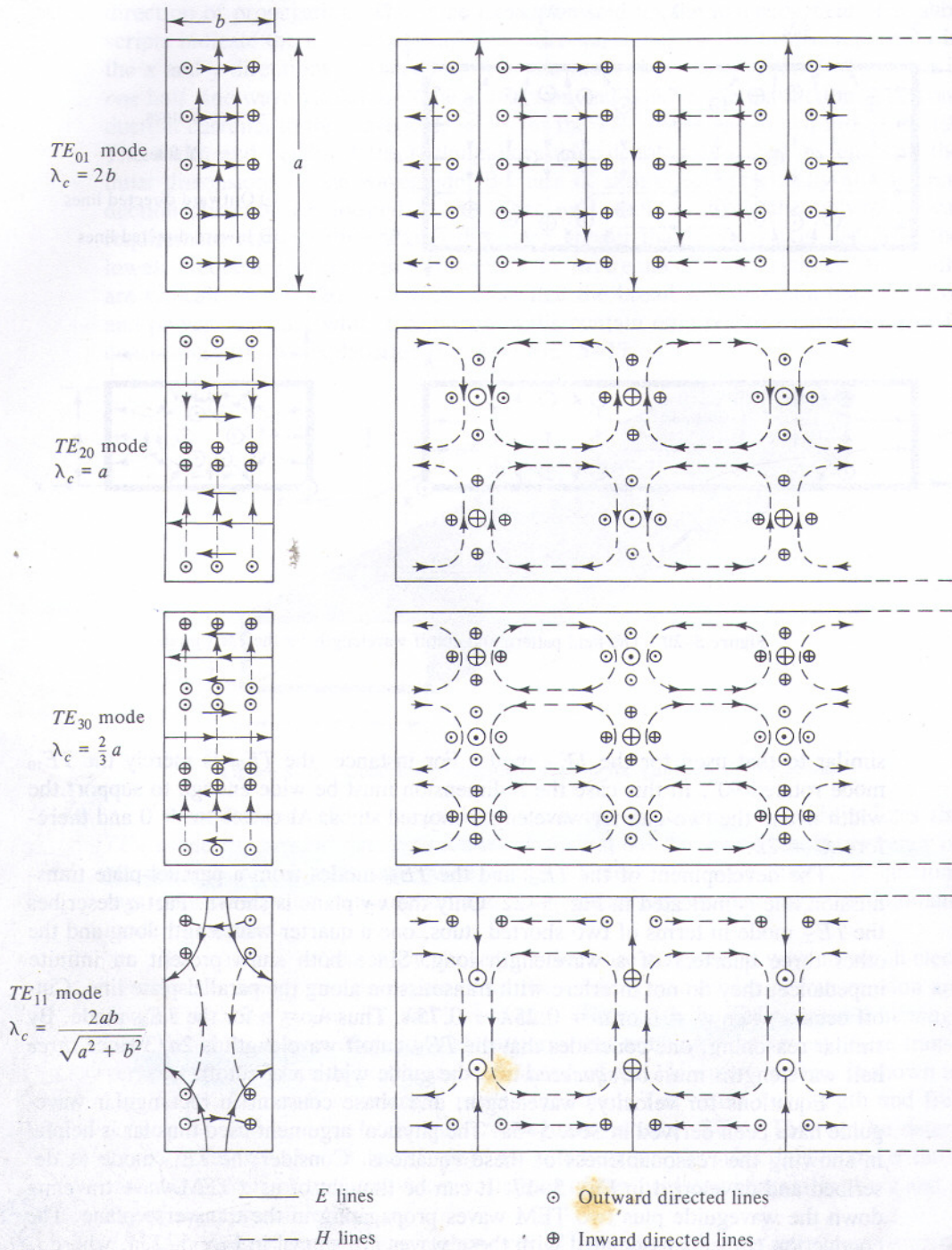


Figure 5-21 Field patterns for some higher-order TE modes in rectangular waveguide. Additional TE and TM modes are described in Chapter 5 of Ref. 5-8.

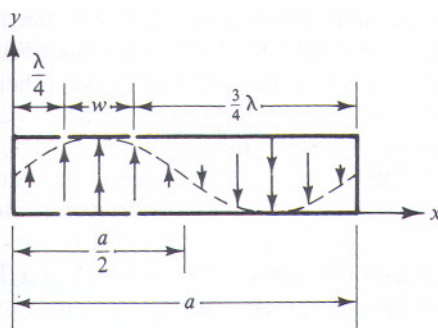
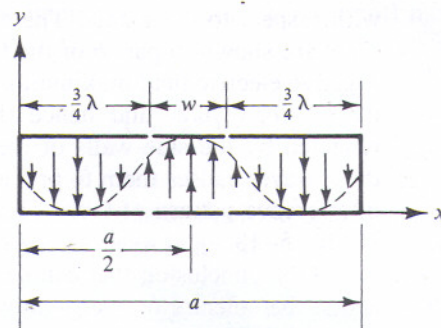
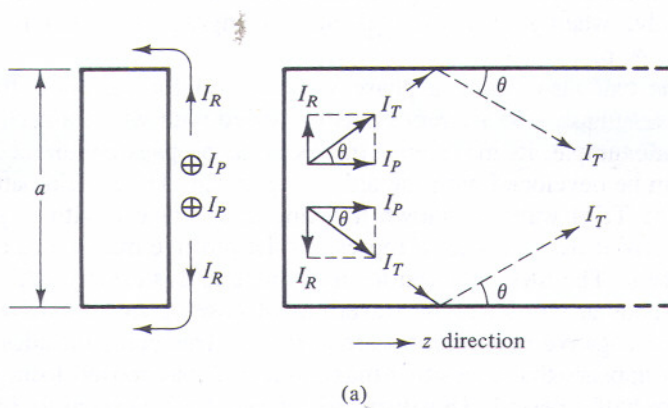
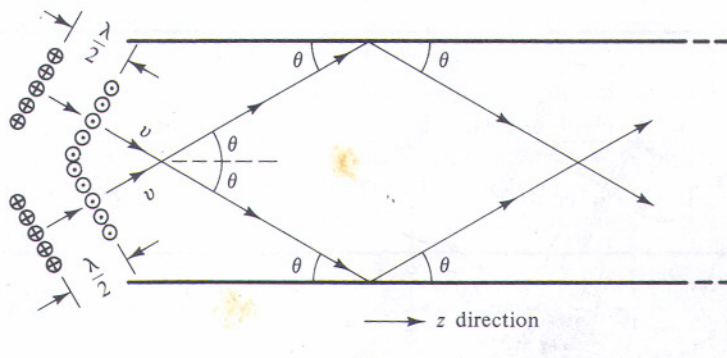
(a) TE_{20} mode(b) TE_{30} mode

Figure 5-22 An explanation of the TE_{20} and TE_{30} modes in terms of shorted stubs and a parallel-plate line.



(a)



(b)

Figure 5-23 The TE_{10} mode as the interference pattern of two TEM waves.

with respect to the z axis. The electromagnetic waves associated with the two currents are shown in part *b* of the figure. For the sake of clarity, only the positive and negative electric field maximums are shown. Since they are TEM waves, their velocity $v = c/\sqrt{\mu_R \epsilon_R}$ and hence the wavelength $\lambda = \lambda_0/\sqrt{\mu_R \epsilon_R}$. These waves are reflected by the side walls of the metal waveguide. The continuing re-reflection of these waves causes them to propagate in the zigzag manner shown in the figure. The interference pattern of these TEM waves results in the TE_{10} mode pattern described in Fig. 5-18.

One conclusion that can be drawn from the above interpretation of a TE wave is that the velocity of energy flow down the waveguide is less than v since the effective length of travel is increased by the zigzag path of the TEM waves. This velocity (v_g) is known as the *group velocity* of the wave. An expression for v_g is given by Eq. (5-74). Since $v_g = v \cos \theta$,

$$\cos \theta = \sqrt{1 - (f_c/f)^2} \quad (5-37)$$

This equation is plausible since at cutoff ($f = f_c$), $\theta = 90^\circ$, which means the power current I_p is zero. Thus at cutoff, the two TEM waves bounce back and forth between the side walls of the guide and hence no energy flows down the waveguide. Conversely, when $f \gg f_c$, $\theta \approx 0$ and the zigzagging effect is negligible, which means $v_g \approx v$.

One can also define a phase velocity (v_p) for the wave traveling down the waveguide. Phase velocity represents the speed with which a particular phase of the wave (for example, its maximum) travels in the propagation direction. An expression for v_p can be developed with the aid of Fig. 5-24. The E -field pattern (at $t = 0$) for one of the TEM waves is shown traveling at an angle θ with respect to the z axis. The wavefront passing point d represents the positive maximums of E traveling with a velocity v . The time required for it to move $\lambda/2$ is exactly $T/2$, where T is the ac period. Thus at $t = T/2$, the wavefront of positive maximums arrive at the plane where the negative maximums were at $t = 0$. This plane includes the point e . As a result, it appears that a positive maximum of E has moved from the point d to the point e in half a period. This distance, labeled $\lambda_g/2$, is equal to $\lambda/(2 \cos \theta)$. There-

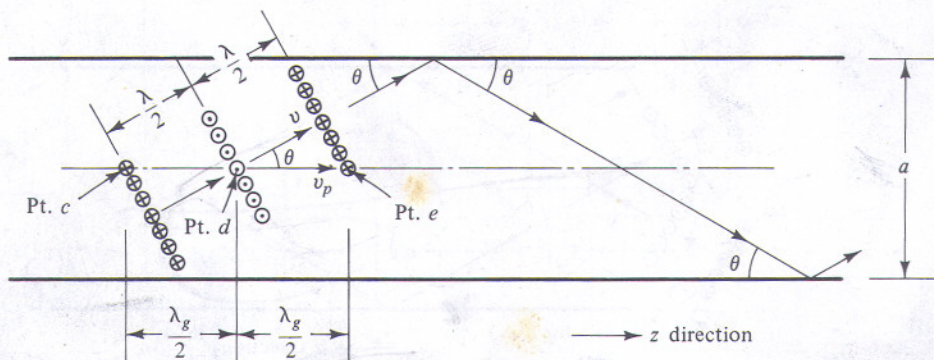


Figure 5-24 A description of phase velocity and guide wavelength in rectangular waveguide.

fore the velocity with which a positive maximum (or any other phase point) moves along the waveguide axis is

$$v_p = \frac{\lambda}{T/2} = \frac{v}{\cos \theta} = \frac{c/\sqrt{\mu_R \epsilon_R}}{\sqrt{1 - (f_c/f)^2}} \quad (5-38)$$

which is exactly Eq. (5-71). Note that v_p can be greater than the speed of light.⁷ This does not contradict relativity theory because there is no energy or information transfer associated with this velocity. On the other hand, v_g must be less than the speed of light since it represents the velocity of energy flow in waveguide. For TEM lines, $f_c = 0$ and hence $v_p = v_g = v$.

Since v_p represents the phase velocity of a steady-state sinusoidal signal, it is related to guide wavelength (λ_g) by $v_p = f\lambda_g$. From Fig. 5-24,

$$\lambda_g = \frac{\lambda}{\cos \theta} = \frac{\lambda}{\sqrt{1 - (f_c/f)^2}} \quad (5-39)$$

or

$$\lambda_g = \frac{\lambda_0}{\sqrt{\mu_R \epsilon_R - (\lambda_0/\lambda_c)^2}} \quad (5-40)$$

which is exactly Eq. (5-70). The phase constant β for the TE mode in the guide is related to v_p and λ_g by

$$\beta = \frac{\omega}{v_p} = \frac{2\pi}{\lambda_g} \quad \text{rad/length} \quad (5-41)$$

Although these expressions [Eqs. (5-38) to (5-41)] have been developed on the basis of TE_{10} mode propagation, they are applicable to any TE or TM mode. The equation for group velocity [Eq. (5-74)] also applies to any mode. The cutoff wavelength (λ_c) and frequency (f_c) for the particular mode can be determined from Eqs. (5-67) and (5-68). For the TE_{10} mode, $m = 1$ and $n = 0$ and hence these equations reduce to Eqs. (5-35) and (5-36), respectively. Note that as the operating frequency approaches cutoff ($f \rightarrow f_c$), $v_g \rightarrow 0$, $v_p \rightarrow \infty$, and $\lambda_g \rightarrow \infty$. A graph of normalized guide wavelength and phase velocity versus normalized frequency is shown in Fig. 5-25. Group velocity is also shown.

At frequencies below the cutoff frequency of a particular mode, the electromagnetic wave is attenuated as it attempts to propagate down the waveguide. When $f < f_c$, the phase constant β is imaginary which implies wave attenuation. When combined with Eq. (5-39), Eq. (5-41) can be rewritten as

$$\beta = j \frac{2\pi}{\lambda} \sqrt{\left(\frac{f_c}{f}\right)^2 - 1} = j \frac{2\pi f_c}{v} \sqrt{1 - \left(\frac{f}{f_c}\right)^2} = j\alpha$$

⁷ Some authors use the analogy of an ocean wave breaking on the shoreline to describe the concept of phase velocity. See, for example, Sec. 5.4 in Ref. 5-8.

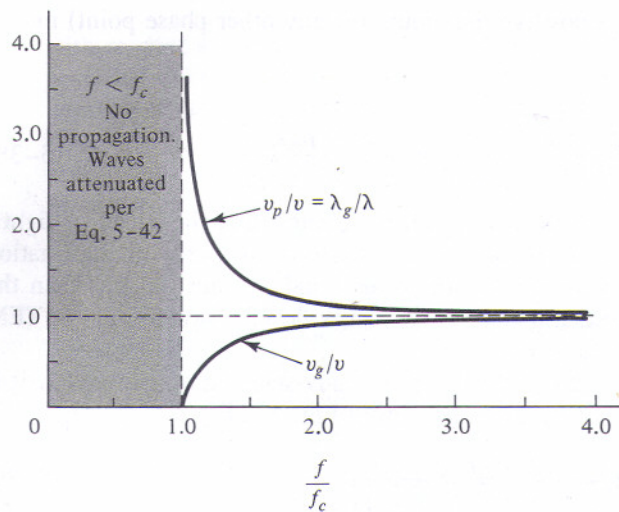


Figure 5-25 The variation of velocity and guide wavelength with frequency.

and hence the attenuation constant due to the cutoff effect is

$$\alpha = \frac{2\pi}{\lambda_c} \sqrt{1 - \left(\frac{f}{f_c}\right)^2} \quad \text{Np/length}$$

or

$$\alpha = \frac{54.6}{\lambda_c} \sqrt{1 - \left(\frac{f}{f_c}\right)^2} \quad \text{dB/length}$$
(5-42)

These expressions are identical to Eq. (5-75) and apply to any TE or TM mode. Since the derivation of these equations assumed a lossless insulator in the waveguide and perfectly conducting guide walls, this attenuation is *not* associated with dissipative losses. In general, the cutoff attenuation manifests itself in a circuit as reflection loss. Conceptually, it is identical to the stopband attenuation of a reactive filter. As stated earlier, a section of waveguide behaves like a highpass filter. When $f > f_c$, the guide exhibits very low loss, while at frequencies below f_c , the attenuation is high which results in practically full reflection (that is, $|\Gamma| \approx 1$).

Waveguide impedance.⁸ In order to use the various analytical techniques developed in Chapters 3 and 4, one usually needs to know the characteristic impedance (Z_0) and wavelength for the particular transmission line. For waveguide, the wavelength is given by Eq. (5-39) or (5-40). As explained in Sec. 5-5a, the characteristic impedance of a waveguide is *not* uniquely defined. The reason is that for a given field pattern, voltage can be defined in a variety of ways. Four possible forms of Z_0 for rectangular waveguide are given in Eqs. (5-79) and (5-81). Unless

⁸ This is not to be confused with *wave impedance* which is defined as the ratio of transverse electric field to transverse magnetic field at any point in the waveguide. For TE and TM modes it is denoted as Z_{TE} and Z_{TM} , respectively.

otherwise stated, the modified power-voltage definition will be used in this text. It is repeated here for convenience.

$$Z_0 = 377 \frac{b}{a} \sqrt{\frac{\mu_R}{\epsilon_R}} \frac{\lambda_g}{\lambda} = \frac{377 \frac{b}{a} \sqrt{\frac{\mu_R}{\epsilon_R}}}{\sqrt{1 - \left(\frac{f_c}{f}\right)^2}} \text{ ohms} \quad (5-43)$$

Problems 5-23 and 5-25 use this form to design quarter-wave transformers in rectangular guide. If any of the other forms of Z_0 were used to solve these problems, the results would be the same! The reason is that the various forms of Z_0 differ only by a constant. Since matching involves the *ratio* of impedances, the value of the constant is immaterial.

When a waveguide must be matched to a uniquely defined impedance (for example, a coaxial line), the choice of Z_0 for the waveguide *does* become material. In this situation, the usual approach is to use whichever definition leads to the best agreement between transmission-line theory and the experimental data (see Ref. 5-30). Of course, once a choice is made, it should be used throughout the particular analysis.

It is interesting to note that below cutoff, Z_0 is imaginary. This can be understood with the aid of Fig. 5-17 since for $f < f_c$, $w = 0$, and $l < \lambda/4$. As a result, the impedance of the shorted stubs is inductive and hence the waveguide impedance is imaginary. The characteristic impedance of a reactive filter behaves similarly in its stopband. In the passband, the L/C ratio of the reactive filter is used to control its characteristic impedance. For waveguides, the dimensions (a, b) or the properties of the insulating material (μ_R, ϵ_R) may be varied to adjust Z_0 .

Some of the waveguide concepts discussed thus far are highlighted in the following illustrative example.

Example 5-1:

A rectangular waveguide (Fig. 5-16) has the following characteristics:

$$b = 1.5 \text{ cm}, \quad a = 3.0 \text{ cm}, \quad \mu_R = 1, \quad \epsilon_R = 2.25.$$

- (a) Calculate the cutoff wavelength and frequency for the TE_{10} , TE_{20} , and TM_{11} modes.
- (b) Calculate λ_g and Z_0 at 4.0 GHz.
- (c) Calculate the attenuation constant (in dB/cm) at 3.0 GHz for the dielectric-filled guide. What is the total attenuation (in dB) if the guide is 12 cm long?
- (d) What is the total attenuation at frequencies much less than the TE_{10} cutoff frequency?

Solution:

- (a) From Eq. (5-67), λ_c equals $2a$, a , and $2ab/\sqrt{a^2 + b^2}$ for the TE_{10} , TE_{20} , and TM_{11} modes, respectively. Thus the cutoff wavelengths are 6.0 cm for TE_{10} , 3.0 cm for TE_{20} , and 2.68 cm for TM_{11} . The cutoff frequencies are a function of the dielec-

tric properties of the insulating material as well as the guide dimensions. From Eq. (5-68),

$$f_c = 3.33 \times 10^9 \text{ Hz or } 3.33 \text{ GHz for the } TE_{10} \text{ mode.}$$

Similarly, $f_c = 6.66 \text{ GHz}$ for the TE_{20} mode and 7.46 GHz for the TM_{11} mode. Assuming $a > b$, the TE_{10} mode always has the lowest cutoff frequency and hence is the dominant mode.

- (b) The guide wavelength is obtained from Eq. (5-40). With $\lambda_0 = 7.5 \text{ cm}$ at 4.0 GHz,

$$\lambda_g = \frac{7.5}{\sqrt{2.25 - \left(\frac{7.5}{6.0}\right)^2}} = 9.05 \text{ cm}$$

where the TE_{10} mode has been assumed.

The characteristic impedance of the guide is calculated from Eq. (5-43). Since $\lambda = 7.5/\sqrt{2.25} = 5.0 \text{ cm}$,

$$Z_0 = 377 \frac{1.5}{3.0} \sqrt{\frac{1}{2.25}} \frac{9.05}{5.0} = 227 \text{ ohms}$$

Note that a reduction in the guide height b lowers the impedance of the waveguide without changing its TE_{10} cutoff frequency. This is useful when changes in impedance level are required in a waveguide system.

- (c) The waveguide is below cutoff to a 3.0 GHz signal and hence the attenuation constant is given by Eq. (5-42). With $\lambda_c = 6.0 \text{ cm}$ for the TE_{10} mode,

$$\alpha = \frac{54.6}{6} \sqrt{1 - \left(\frac{3.0}{3.33}\right)^2} = 3.95 \text{ dB/cm}$$

and

$$A_t = \alpha l = (3.95)(12) = 47.4 \text{ dB}$$

When the guide is operating below cutoff, its characteristic impedance is imaginary. Therefore, the above figure only approximates the insertion loss of the 12 cm section in a system with Z_G and Z_L real. (The difference between L_t and A_t is explained in Sec. 4-3a.) The calculation of L_t from A_t is described in Sec. 3.07 of Ref. 5-10.

- (d) When $f \ll f_c$,

$$\alpha \approx \frac{54.6}{\lambda_c} \text{ dB/length} \quad \text{or} \quad A_t \approx \frac{54.6}{\lambda_c} l \text{ dB.}$$

Therefore,

$$A_t = \frac{54.6}{6} (12) = 109.2 \text{ dB.}$$

Note that if the above inequality holds for the dominant mode, then α and A_t are independent of frequency for all modes.

Power handling capacity of rectangular waveguide. The maximum power that a coaxial line can transmit before the onset of voltage breakdown was discussed in Sec. 5-2. Equation (5-21) describes how this value is related to the

maximum usable frequency and the dielectric strength of the insulator. The following discussion shows that the power handling capacity of rectangular waveguide is significantly greater.

For the TE_{10} mode, the largest electric field occurs along the center line of the broad wall ($x = a/2$). This is shown in Fig. 5-18 and is given above Eq. (5-77). Since this equation gives the rms value, the peak value is $\sqrt{2}E_0\lambda_c/\lambda_g$. To avoid voltage breakdown,

$$\sqrt{2}E_0 \frac{\lambda_c}{\lambda_g} \leq E_d$$

where E_d is the dielectric strength of the insulating material in the waveguide. From Eq. (5-80),

$$P = \frac{ab}{2Z_{TE}} \left(E_0 \frac{\lambda_c}{\lambda_g} \right)^2 \leq \frac{ab}{4Z_{TE}} E_d^2$$

where $E_0 = H_0 Z_{TE}$ and Z_{TE} is defined by Eq. (5-63). Thus for the TE_{10} mode, the maximum power capability of rectangular guide is

$$P_{\max} = \frac{ab}{4Z_{TE}} E_d^2 \quad (5-44)$$

Choosing a and b as large as possible will, of course, maximize P_{\max} . However, as explained earlier (Sec. 5-2), it is desirable that only the dominant mode be allowed to propagate. To prevent higher-mode propagation, the operating frequency must be less than the cutoff frequency of the TE_{20} mode. Defining f_{\max} as 0.95 of this value yields

$$f_{\max} = \frac{0.95c}{a\sqrt{\mu_R \epsilon_R}} \quad (5-45)$$

To prevent possible TE_{01} mode propagation at frequencies below f_{\max} , the guide height is chosen so that $b \leq a/2$. With this restriction, the cutoff frequency of the TE_{01} mode is equal to or greater than that of the TE_{20} , and thus the above equation defines the upper frequency limit of the guide. Setting $b = a/2$ and assuming an air-filled rectangular waveguide results in the following equation for maximum power handling capacity.

$$P_{\max} = 27 \left(\frac{E_d}{f_{\max}} \right)^2 \sqrt{1 - \left(\frac{f_c}{f} \right)^2} \quad \text{watts} \quad (5-46)$$

where f_{\max} is in MHz, E_d in V/m, f_c is the TE_{10} cutoff frequency, and f is the operating frequency. Since $f_c \approx 0.5f_{\max}$, f_c/f generally ranges from 0.5 to 0.8. By comparing this equation with that for an air-filled coaxial line [Eq. (5-21)], it is apparent that the power handling capacity of waveguide is significantly greater.

To get an idea of its power capacity, consider a 1 cm by 2 cm air-filled rectangular guide. From Eq. (5-45), $f_{\max} = 14,250$ MHz. At room temperature and a pressure of one atmosphere, $E_d = 3 \times 10^6$ V/m. Assuming an operating frequency of 12,000 MHz, $P_{\max} = 934$ kW since $f_c = 7500$ MHz for the TE_{10} mode. Allowing

for the possibility of large standing waves, the actual power capacity is one-fourth the above value. As mentioned at the end of Sec. 5-2, P_{\max} can be increased by pressurizing the air in the waveguide.

Dissipative attenuation in rectangular waveguide. Unlike the below-cutoff attenuation described earlier, this attenuation is associated with dissipative losses in the waveguide walls and the insulating material within the guide. The attenuation constant due to an imperfect, nonmagnetic dielectric in the waveguide is given by

$$\alpha_d = \frac{27.3 \sqrt{\epsilon_R} \tan \delta}{\lambda_0 \sqrt{1 - (f_c/f)^2}} \quad \text{dB/length} \quad (5-47)$$

where $\tan \delta$ is the dielectric loss tangent of the insulating material. Note that except for the cutoff term $\sqrt{1 - (f_c/f)^2}$, the expression for α_d is the same as for TEM lines. Since the cutoff term equals $\cos \theta$, the resultant increase in α_d can be interpreted as due to the zigzagging of the two TEM waves as they travel down the guide.

For TE_{10} mode propagation, the attenuation constant associated with imperfect conducting walls is given by

$$\alpha_c = \frac{R_s}{b\eta} \frac{1 + \frac{2b}{a} \left(\frac{f_c}{f}\right)^2}{\sqrt{1 - (f_c/f)^2}} \quad \text{Np/length} \quad (5-48)$$

where $\eta = 377 \sqrt{\mu_R/\epsilon_R}$, $R_s = 1/(\sigma\delta_s)$ and f_c is the TE_{10} cutoff frequency. The above equations are derived in Chapter 8 of Ref. 5-6.

In most applications, the waveguide is air-filled ($\alpha_d = 0$) and therefore the total attenuation constant is simply α_c . This attenuation is considerably less than that in a comparable coaxial line, which is another advantage of waveguide transmission.

With $\eta = 377$ ohms for air and δ_s given by Eq. (2-73), the above equation can be written as

$$\alpha_c = 27.3 \frac{\delta_s}{\lambda_0 b} \frac{1 + \frac{2b}{a} \left(\frac{f_c}{f}\right)^2}{\sqrt{1 - (f_c/f)^2}} \quad \text{dB/length} \quad (5-49)$$

where nonmagnetic waveguide walls have been assumed. Curves of α_c versus frequency for $a = 2.0$ cm are shown in Fig. 5-26 for three values of b/a . It is apparent from the data that increasing the guide height b reduces the attenuation. However, as explained below Eq. (5-45), it is necessary that $b \leq a/2$. Letting $b = a/2$ and utilizing Eq. (5-45) reduces the above expression for α_c to

$$\alpha_c = 0.19 \frac{\delta_s}{\lambda_0} f_{\max} \left\{ \frac{1 + (f_c/f)^2}{\sqrt{1 - (f_c/f)^2}} \right\} \quad \text{dB/m} \quad (5-50)$$

where f_{\max} is in MHz and, as noted earlier, $f_c \approx 0.5 f_{\max}$. Except when f approaches f_c , the value of the bracketed term is about 1.5 to 2.0. A comparison of Eqs. (5-50) and (5-20) verifies that for a given value of f_{\max} , an air-filled rectangular guide has significantly lower loss than a coaxial line.

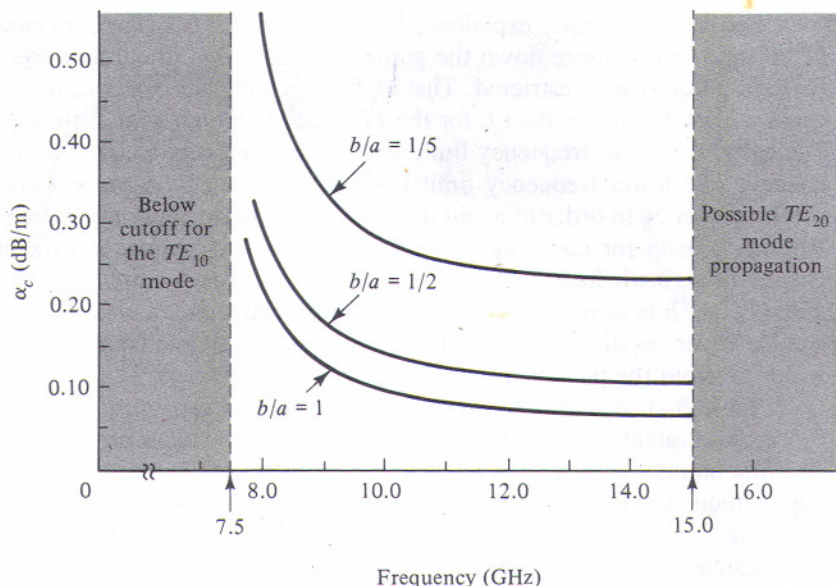


Figure 5-26 TE_{10} mode attenuation for air-filled rectangular guide with copper walls. Guide width $a = 2.0$ cm.

Standard dimensions for rectangular waveguides. As the microwave industry matured, the need for a set of standard waveguide sizes for the various frequency bands became apparent. A complete listing of standard air-filled rectangular waveguides may be found in the Microwave Engineers' Handbook (Ref. 5-4). Table 5-1 lists some of them and their recommended frequency ranges. Note that the useful bandwidth in all cases is approximately 40 percent or half an octave. Also, the dimensional aspect ratio (a/b) is roughly two. The reason the ratios are not exactly two is that most guide sizes were chosen on the basis of extrusions that were readily available during World War II.

TABLE 5-1 Standard rectangular waveguide sizes as recommended by the Electronic Industries Association (EIA)

EIA Designation	Usable Frequency Range (GHz)	Inner Dimensions $b \times a$ (inches)	Attenuation* (dB/100 ft.)	Peak Power Capacity (Kilowatts)
WR-284	2.60–3.95	1.340×2.840	1.10–0.75	2200–3200
WR-187	3.95–5.85	0.872×1.872	2.08–1.44	1400–2000
WR-137	5.85–8.20	0.622×1.372	2.87–2.30	560–710
WR-90	8.20–12.40	0.400×0.900	6.45–4.48	200–290
WR-62	12.40–18.00	0.311×0.622	9.51–8.31	120–160
WR-42	18.00–26.50	0.170×0.420	20.7–14.8	43–58

* Theoretical values for brass waveguide.

For reasons already explained, it is desirable that only the dominant TE_{10} mode be allowed to propagate down the guide. To insure this, the usable frequency range for each guide size is restricted. That is, for a given guide width a , the operating frequency must be greater than f_c for the TE_{10} mode and less than f_c for the TE_{20} mode. Typically, the upper frequency limit is set about 5 percent below the TE_{20} cutoff frequency. The lower frequency limit is set approximately 25 percent above the TE_{10} cutoff frequency in order to avoid the high attenuation region near f_c (see Fig. 5-26). Another reason for choosing the lower limit in this manner is to avoid the rapid change of λ_g with frequency that occurs near f_c (Fig. 5-25). The choice of waveguide height b is governed by the desire for low attenuation and high power capability. However, as discussed earlier, the guide height should be no more than half the width to avoid the possibility of TE_{01} mode propagation.

Table 5-1 also lists the attenuation and power capability for each guide size. Since these quantities are frequency dependent, two values are given in each case. The first number indicates its value at the lower frequency limit and the second at the upper frequency limit. The power capacity figures include safety factors for manufacturing imperfections and the possible existence of standing waves along the guide. The attenuation values listed are for brass waveguides. Note that the higher the frequency range of interest, the smaller the guide size, which results in higher attenuation and lower power handling capacity.

5-4b Circular Waveguide

When rectangular guide is used within its recommended frequency range, the plane of polarization of the propagating wave is uniquely defined. As shown in Fig. 5-18, the electric field is directed across the narrow dimension of the waveguide. There are certain applications, however, that require dual polarization capability. For example, a waveguide connected to a circularly-polarized antenna must be able to efficiently propagate both vertically and horizontally polarized waves. A square waveguide has this capability since with $b = a$, the cutoff frequencies for the TE_{10} and TE_{01} modes are the same. To insure that only these modes can propagate, the upper frequency limit is usually set 5 percent below the cutoff frequency of the TM_{11} mode. For square guide, the TM_{11} cutoff frequency is lower than the TE_{20} and hence determines the upper frequency limit. As before, the lower limit is set about 25 percent above the cutoff frequency of the TE_{10} (and TE_{01}) mode.

Circular waveguide is the most common form of a dual-polarization transmission line. Like rectangular waveguide, it has an infinite set of TE and TM modes. The theoretical analysis detailed in Sec. 5-5b yields the field patterns and the cutoff wavelengths for the various modes. Four of the most important modes and their cutoff wavelengths are given in Fig. 5-27. Only the field patterns in the transverse plane are shown. The coefficients in the expressions for λ_c are related to the zeros of certain Bessel functions and their derivatives. Some of these coefficients are also listed in Sec. 5-5b (Table 5-3). Additional modes and their cutoff wavelengths may be found in Refs. 5-6, 5-8, and 5-9. The first mode subscript indicates the number of full sine wave variations in the circumferential direction, while the second is related to the Bessel function variations in the radial direction.

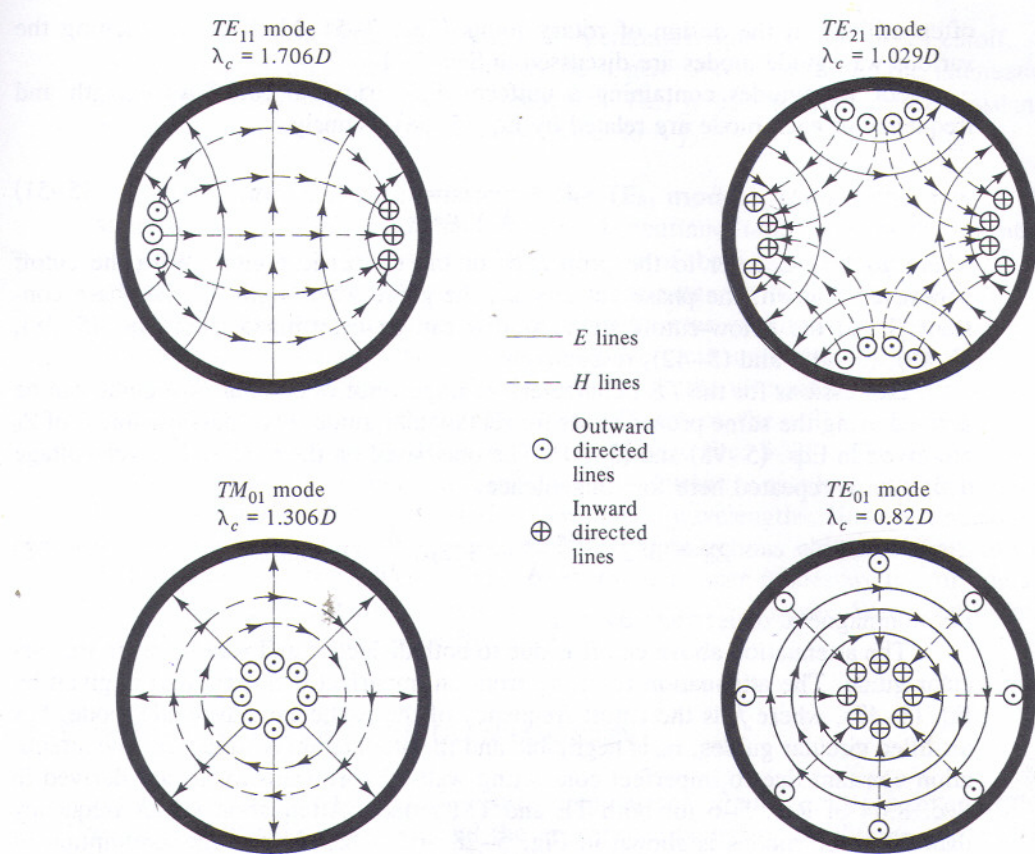


Figure 5-27 The transverse field patterns for some common circular waveguide modes. D = inner guide diameter.

Since the TE_{11} mode has the lowest cutoff frequency, it is the dominant mode in circular guide. Its electric and magnetic field pattern is similar to the TE_{10} in square guide. That is, if one imagines a gradual changing of the guide cross section from square to round, the TE_{10} mode in square guide becomes the TE_{11} mode in circular guide. In like manner, the TM_{01} mode in circular guide is analogous to the TM_{11} mode in square guide. The upper frequency limit of circular guide is restricted by the TM_{01} mode, since its cutoff frequency is the lowest of the higher-order modes.⁹ It is interesting to note the similarity between the TM_{01} mode in circular guide and the TEM mode in a coaxial line. The only substantial difference is that the conduction current in the center conductor of the coaxial line is replaced by a displacement current associated with the longitudinal electric field (E_z) along the axis of the round guide. Modes with circular symmetry, such as the TM_{01} and TE_{01} , are

⁹ In most waveguide transmission systems, energy conversion from the dominant TE_{11} mode to the TM_{01} mode is rare. Therefore, the upper frequency limit of circular guide is usually defined as 95 percent of the TE_{21} cutoff frequency.

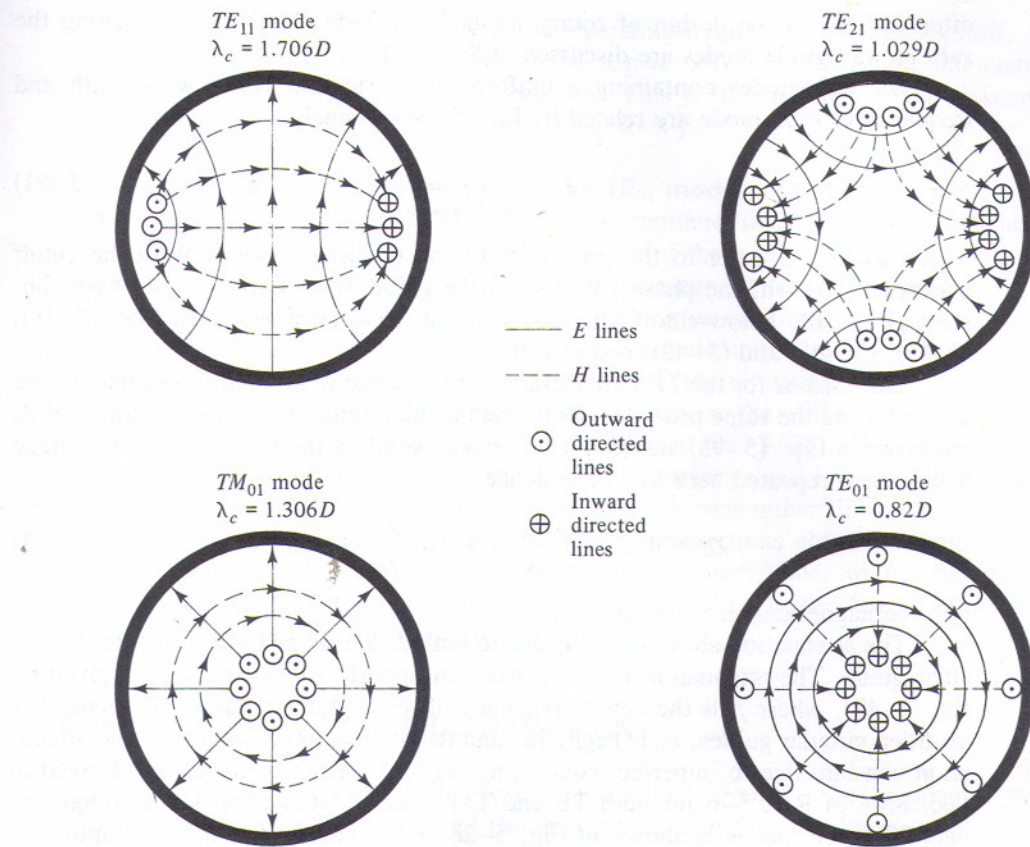


Figure 5-27 The transverse field patterns for some common circular waveguide modes. D = inner guide diameter.

Since the TE_{11} mode has the lowest cutoff frequency, it is the dominant mode in circular guide. Its electric and magnetic field pattern is similar to the TE_{10} in square guide. That is, if one imagines a gradual changing of the guide cross section from square to round, the TE_{10} mode in square guide becomes the TE_{11} mode in circular guide. In like manner, the TM_{01} mode in circular guide is analogous to the TM_{11} mode in square guide. The upper frequency limit of circular guide is restricted by the TM_{01} mode, since its cutoff frequency is the lowest of the higher-order modes.⁹ It is interesting to note the similarity between the TM_{01} mode in circular guide and the TEM mode in a coaxial line. The only substantial difference is that the conduction current in the center conductor of the coaxial line is replaced by a displacement current associated with the longitudinal electric field (E_z) along the axis of the round guide. Modes with circular symmetry, such as the TM_{01} and TE_{01} , are

⁹ In most waveguide transmission systems, energy conversion from the dominant TE_{11} mode to the TM_{01} mode is rare. Therefore, the upper frequency limit of circular guide is usually defined as 95 percent of the TE_{21} cutoff frequency.

often utilized in the design of rotary joints (Sec. 7-5). Methods for exciting the various waveguide modes are discussed in Sec. 7-1.

For waveguides containing a uniform dielectric, the cutoff wavelength and frequency of each mode are related by Eq. (5-68). Namely,

$$f_c = \frac{c}{\lambda_c \sqrt{\mu_R \epsilon_R}} \quad (5-51)$$

where μ_R and ϵ_R refer to the properties of the dielectric region. With the cutoff parameters known, the phase velocity v_p , the guide wavelength λ_g , the phase constant β and the below-cutoff attenuation α can be determined from Eqs. (5-38), (5-40), (5-41), and (5-42), respectively.

Expressions for the TE_{11} characteristic impedance of circular waveguide can be derived using the same procedure as for rectangular guide. Four possible forms of Z_0 are given in Eqs. (5-98) and (5-99). The one based on the modified power-voltage definition is repeated here for convenience.

$$Z_0 = 382 \sqrt{\frac{\mu_R}{\epsilon_R} \frac{\lambda_g}{\lambda}} = 382 \mu_R \frac{\lambda_g}{\lambda_0} \text{ ohms} \quad (5-52)$$

For nonmagnetic dielectrics, $\mu_R = 1$.

The attenuation above cutoff is due to both dielectric and wall losses in the circular guide. The attenuation resulting from an imperfect dielectric (α_d) is given by Eq. (5-47), where f_c is the cutoff frequency of the particular waveguide mode. For air-filled circular guides, α_d is negligible and the attenuation is simply α_c , the attenuation constant due to imperfect conducting walls. Expressions for α_c are derived in Sec. 8.04 of Ref. 5-6 for both TE and TM modes. Attenuation versus frequency data for three modes is shown in Fig. 5-28 and is based upon the assumption of copper walls and a guide diameter of 3 cm. The general attenuation behavior for the TE_{11} and TM_{01} modes is about the same as for the TE_{10} mode in rectangular guide.

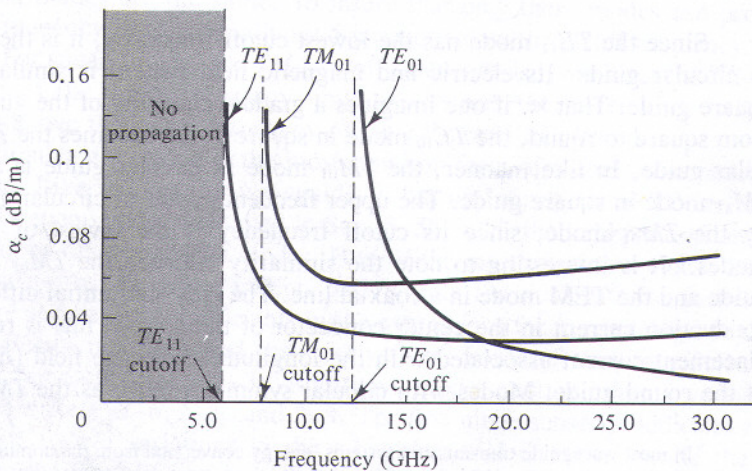


Figure 5-28 Attenuation for air-filled circular guide with a copper wall. Guide diameter $D = 3.0$ cm.

The attenuation increases rapidly as the operating frequency approaches cutoff. An explanation for this effect has already been given. When $f \gg f_c$, the attenuation increases slowly with increasing frequency. This is because the surface resistance R_s associated with skin effect is proportional to \sqrt{f} .

Attenuation characteristics of the TE_{01} mode. Unlike other modes, the attenuation of the TE_{01} mode in circular guide continues to decrease as the operating frequency increases. This is due to the behavior of the conduction currents with increasing frequency. Referring to Fig. 5-27, the magnetic field at the guide walls is everywhere longitudinal for the TE_{01} mode. By virtue of Ampere's right-hand rule, this means that the wall currents are completely circumferential. Furthermore, a field analysis shows that for a fixed power level, the circumferential currents decrease with increasing frequency (Ref. 5-6). Therefore, the wall losses and hence α_c decrease indefinitely as the frequency increases (see Fig. 5-28). This characteristic of the TE_{01} mode in circular guide makes it very attractive as a low-loss transmission line at high frequencies, particularly at millimeter wavelengths. However, since it is not the dominant mode, one must take special precautions not to generate modes with a lower cutoff frequency. The generation of other modes would, of course, result in a significant loss of power in the desired TE_{01} mode. Some results and problem areas are described in Ref. 5-31.

★ 5-5 THEORY OF WAVEGUIDE TRANSMISSION

An analysis of wave transmission in rectangular and circular guides is given in this section. Maxwell's equations and the appropriate boundary conditions are used to develop the field equations for the various modes. Also obtained are expressions for cutoff, velocity, wavelength, and characteristic impedance.

In developing the field equations, it is assumed that the guide walls are perfect conductors and the region inside the waveguide is a perfect insulator. Therefore, conduction currents are confined to the inner wall surfaces and hence the wall thickness does not enter into the analysis. Further, it is assumed that the waveguide extends infinitely in both the plus and minus z direction.

For sinusoidal excitation, Maxwell's equations [Eqs. (2-38) to (2-40)] in a charge-free dielectric region may be written in phasor form. That is,

$$\nabla \cdot \vec{D} = 0, \quad \nabla \cdot \vec{B} = 0, \quad \nabla \times \vec{E} = -j\omega \vec{B}, \quad \text{and} \quad \nabla \times \vec{H} = j\omega \vec{D}$$

since ρ_v and \vec{J} are zero in the dielectric. Faraday and Ampere's laws may be rewritten as

$$\nabla \times \vec{E} = -j\omega \mu_R \mu_0 \vec{H} \quad \text{and} \quad \nabla \times \vec{H} = j\omega \epsilon_R \epsilon_0 \vec{E} \quad (5-53)$$

since $\vec{D} = \epsilon_R \epsilon_0 \vec{E}$ and $\vec{B} = \mu_R \mu_0 \vec{H}$. The constants μ_R and ϵ_R define the electric and magnetic properties of the dielectric region. Taking the curl of both sides of the first equation and using the vector identity, $\nabla \times \nabla \times \vec{A} = \nabla(\nabla \cdot \vec{A}) - \nabla^2 \vec{A}$ yields

$$\nabla(\nabla \cdot \vec{E}) - \nabla^2 \vec{E} = -j\omega \mu_R \mu_0 \nabla \times \vec{H}$$

where it has been assumed that the dielectric is linear, homogeneous, and isotropic.

Using Ampere's law,

$$\nabla^2 \vec{E} + \omega^2 \mu_R \mu_0 \epsilon_R \epsilon_0 \vec{E} = 0 \quad (5-54)$$

since $\nabla \cdot \vec{E} = 0$. In a similar manner,

$$\nabla^2 \vec{H} + \omega^2 \mu_R \mu_0 \epsilon_R \epsilon_0 \vec{H} = 0 \quad (5-55)$$

These are known as the *vector wave equations* for the electric and magnetic fields in a charge-free region. They will now be used to obtain the field equations in rectangular and circular waveguides.

5-5a Rectangular Waveguide Transmission

Figure 5-16 shows a rectangular waveguide of height b and width a . This is the most common configuration for waveguide transmission. Typically, the dielectric region is air. The coordinate system used in the following analysis is shown in the figure.

In rectangular coordinates, Eq. (5-54) becomes

$$\frac{\partial^2 \vec{E}}{\partial x^2} + \frac{\partial^2 \vec{E}}{\partial y^2} + \frac{\partial^2 \vec{E}}{\partial z^2} + \omega^2 \mu \epsilon \vec{E} = 0$$

where $\mu \equiv \mu_R \mu_0$ and $\epsilon \equiv \epsilon_R \epsilon_0$. For lossless propagation in the positive z direction, all three components of \vec{E} must have an $e^{-j\beta z}$ functional dependence. Therefore

$$\frac{\partial^2 \vec{E}}{\partial x^2} + \frac{\partial^2 \vec{E}}{\partial y^2} + (\omega^2 \mu \epsilon - \beta^2) \vec{E} = 0 \quad (5-56)$$

Similarly,

$$\frac{\partial^2 \vec{H}}{\partial x^2} + \frac{\partial^2 \vec{H}}{\partial y^2} + (\omega^2 \mu \epsilon - \beta^2) \vec{H} = 0 \quad (5-57)$$

This pair of vector equations can be written as six scalar equations by separately equating the x , y , and z components to zero. For the z components,

$$\frac{\partial^2 E_z}{\partial x^2} + \frac{\partial^2 E_z}{\partial y^2} = -k_c^2 E_z \quad (5-58)$$

and

$$\frac{\partial^2 H_z}{\partial x^2} + \frac{\partial^2 H_z}{\partial y^2} = -k_c^2 H_z \quad (5-59)$$

where $k_c^2 \equiv \omega^2 \mu \epsilon - \beta^2$.

It can be shown that the TEM mode cannot exist in a single-conductor transmission system (see Sec. 3.6 of Ref. 5-12). Since rectangular waveguide is in this category, E_z and H_z cannot both be zero. However, if the dielectric medium is uniform, modes can exist with one of the z components equal to zero. When $E_z \equiv 0$, the modes are called TE modes since the electric field is always transverse to the propagation direction. Similarly, those with $H_z \equiv 0$ are called TM modes. Let us now consider both these cases.

With some algebraic manipulation, all the field components can be expressed in terms of \mathbf{H}_z . Namely,

$$\begin{aligned} \mathbf{E}_x &= -j \frac{\omega\mu}{k_c^2} \frac{\partial \mathbf{H}_z}{\partial y}, & \mathbf{E}_y &= j \frac{\omega\mu}{k_c^2} \frac{\partial \mathbf{H}_z}{\partial x} \\ \mathbf{H}_x &= \mp \frac{\mathbf{E}_y}{Z_{TE}}, & \mathbf{H}_y &= \pm \frac{\mathbf{E}_x}{Z_{TE}} \end{aligned} \quad (5-62)$$

where the upper signs are for plus z -directed waves and the lower signs for the minus z -directed waves. Z_{TE} is the *wave impedance* for TE waves. It represents the ratio of transverse electric to transverse magnetic field at any point in the waveguide and is given by

$$Z_{TE} = \frac{\omega\mu}{\beta} = \frac{\eta}{\sqrt{1 - (\lambda/\lambda_c)^2}} \quad \text{ohms} \quad (5-63)$$

where λ_c , the cutoff wavelength, is obtained from Eq. (5-67). The reader is cautioned not to confuse *wave impedance* (Z_{TE}) with *waveguide impedance* (Z_0), which will be described shortly. With $k_x = m\pi/a$ and $k_y = n\pi/b$, k_c^2 may be written as

$$k_c^2 \equiv k_x^2 + k_y^2 = \left(\frac{m\pi}{a}\right)^2 + \left(\frac{n\pi}{b}\right)^2 \quad (5-64)$$

By substituting Eq. (5-61) into Eq. (5-62), the transverse field components of the TE modes for plus z -directed waves are obtained.

$$\begin{aligned} \mathbf{E}_x &= jH_0 \frac{\omega\mu}{k_c^2} \frac{n\pi}{b} e^{-j\beta z} \cos \frac{m\pi}{a} x \sin \frac{n\pi}{b} y \\ \mathbf{E}_y &= -jH_0 \frac{\omega\mu}{k_c^2} \frac{m\pi}{a} e^{-j\beta z} \sin \frac{m\pi}{a} x \cos \frac{n\pi}{b} y \\ \mathbf{H}_x &= -\frac{\mathbf{E}_y}{Z_{TE}} \quad \text{and} \quad \mathbf{H}_y = \frac{\mathbf{E}_x}{Z_{TE}} \end{aligned} \quad (5-65)$$

where H_0 is a constant that indicates the amplitude of the electromagnetic wave. The time-varying form of the field components can be obtained by multiplying the above phasors by $\sqrt{2}e^{j\omega t}$ and taking the real part thereof.

Since $\beta^2 = \omega^2\mu\epsilon - k_c^2$, the phase constant of the wave is

$$\beta = \sqrt{\omega^2\mu\epsilon - \left(\frac{2\pi}{\lambda_c}\right)^2} \quad (5-66)$$

where

$$\lambda_c \equiv \frac{2\pi}{k_c} = \frac{1}{\sqrt{\left(\frac{m}{2a}\right)^2 + \left(\frac{n}{2b}\right)^2}} \quad (5-67)$$

The following discussion explains the meaning of cutoff wavelength (λ_c) and cutoff frequency (f_c).

The integers m and n can take on all values from zero to infinity. Therefore, Eqs. (5-61) and (5-65) represent an infinite set of solutions. Each set of values for m and n describes a method or *mode* of transmitting electromagnetic energy down the rectangular waveguide. The particular TE mode is designated by the symbol TE_{mn} (or by H_{mn} in some texts) and its propagation characteristics are given by Eqs. (5-66) and (5-67). Referring to Eq. (5-65), the subscripts m and n indicate the number of *half* sine wave variations of the field components in the x and y directions, respectively. For a given mode, propagation can only occur when β is real, which requires that $\omega^2 \mu \epsilon > (2\pi/\lambda_c)^2$. This condition for propagation can be rewritten as

$$\lambda < \lambda_c \quad \text{or} \quad f > f_c$$

where f_c , the cutoff frequency, is given by

$$f_c = \frac{v}{\lambda_c} = \frac{c}{\lambda_c \sqrt{\mu_R \epsilon_R}} \quad (5-68)$$

Thus for a given mode, wave propagation only occurs when the signal frequency f is greater than the cutoff frequency. Both λ_c and f_c are dependent upon the dimensions of the waveguide as well as the particular mode being considered. The cutoff frequency (but not λ_c) is also a function of the dielectric material within the guide.

For a given mode, both the phase velocity (v_p) and wavelength in the guide (λ_g) are related to the phase constant. Namely,

$$\beta = \frac{\omega}{v_p} = \frac{2\pi}{\lambda_g} \quad \text{rad/length} \quad (5-69)$$

Using Eq. (5-66) yields

$$\lambda_g = \frac{\lambda_0}{\sqrt{\mu_R \epsilon_R - \left(\frac{\lambda_0}{\lambda_c}\right)^2}} = \frac{\lambda}{\sqrt{1 - \left(\frac{f_c}{f}\right)^2}} \quad (5-70)$$

where λ_0 is the free space wavelength of the signal, $\lambda = \lambda_0 / \sqrt{\mu_R \epsilon_R}$ and λ_c and f_c are defined above. Note that wavelength in the guide is always greater than the wavelength in the unbounded dielectric (λ) since $f > f_c$. The phase velocity in the waveguide is given by

$$v_p = f \lambda_g = \frac{c}{\sqrt{\mu_R \epsilon_R}} \frac{c}{\sqrt{1 - \left(\frac{f_c}{f}\right)^2}} \quad (5-71)$$

Note that it is greater than the wave velocity in an unbounded dielectric. Phase velocity represents the speed with which a particular phase of the wave (such as, its maximum) travels in the propagation direction. With $f\lambda = v$, Eq. (5-71) can be written as

$$v_p = v \frac{\lambda_g}{\lambda} = c \frac{\lambda_g}{\lambda_0} \quad (5-72)$$

where v is the velocity in the unbounded dielectric medium.

One can also define another velocity, known as *group velocity*, in the following manner.

$$v_g \equiv \frac{d\omega}{d\beta} = \frac{1}{d\beta/d\omega} \quad (5-73)$$

This velocity is associated with the propagation of a narrowband modulated signal. It can be shown that the velocity of energy flow in a waveguide is exactly the group velocity (Sec. 3.11 of Ref. 5-12). By substituting Eq. (5-66) into Eq. (5-73), we obtain

$$v_g = \frac{c}{\sqrt{\mu_R \epsilon_R}} \sqrt{1 - \left(\frac{f_c}{f}\right)^2} = v \frac{\lambda}{\lambda_g} \quad (5-74)$$

Note that as $f_c \rightarrow 0$, $v_g = v_p = v$. This is the situation for TEM waves because they do not exhibit the cutoff effect. From Eq. (5-74), it is clear that the velocity of energy flow is always less than the speed of light. This, of course, is consistent with the theory of relativity. Phase velocity, on the other hand, can be greater than the speed of light since it is not the velocity of energy flow or information transfer.

At frequencies below the cutoff frequency ($f < f_c$), the phase constant is imaginary and the electromagnetic wave is attenuated as it attempts to propagate in the z direction. Thus the waveguide behaves like a highpass filter. Since perfect conducting walls have been assumed, the attenuation is reflective rather than dissipative. The expression for this attenuation derives directly from Eq. (5-66). With $\beta = j\alpha$,

$$\alpha = \sqrt{\left(\frac{2\pi}{\lambda_c}\right)^2 - \omega^2 \mu \epsilon}$$

where α represents the attenuation constant of the below-cutoff waveguide. This expression can be rewritten as

$$\alpha = \frac{2\pi}{\lambda_c} \sqrt{1 - \left(\frac{f}{f_c}\right)^2} \quad \text{Np/length} \quad (5-75)$$

or

$$\alpha = \frac{54.6}{\lambda_c} \sqrt{1 - \left(\frac{f}{f_c}\right)^2} \quad \text{dB/length}$$

Note that for $f \ll f_c$, the attenuation constant is independent of frequency.

The most commonly used mode in rectangular waveguide is the TE_{10} . It is called the *dominant mode* because it has the lowest cutoff frequency. Assuming $a > b$, λ_c will have its largest value and f_c its lowest value when $m = 1$ and $n = 0$. The solution wherein both m and n are zero is a trivial case, that is, all field components are zero. The instantaneous field components for the TE_{10} mode are obtained from Eqs. (5-61) and (5-65) by multiplying by $\sqrt{2}e^{j\omega t}$ and taking the real part

thereof. The results for a plus z -directed wave are

$$\mathcal{E}_z \equiv 0, \quad \mathcal{E}_x = 0, \quad \mathcal{H}_y = 0,$$

$$\mathcal{H}_z = \sqrt{2} H_0 \cos \frac{\pi}{a} x \cos(\omega t - \beta z)$$

$$\mathcal{E}_y = \sqrt{2} H_0 \frac{\pi \omega \mu}{ak_c^2} \sin \frac{\pi}{a} x \sin(\omega t - \beta z)$$

and

$$\mathcal{H}_x = -\frac{\mathcal{E}_y}{Z_{TE}}$$

where Z_{TE} is defined in Eq. (5-63).

After some algebraic manipulation, the three field components of the TE_{10} mode reduce to

$$\begin{aligned}\mathcal{E}_y &= \sqrt{2} E_0 \frac{\lambda_c}{\lambda_g} \sin \frac{\pi}{a} x \sin(\omega t - \beta z) \\ \mathcal{H}_x &= -\sqrt{2} H_0 \frac{\lambda_c}{\lambda_g} \sin \frac{\pi}{a} x \sin(\omega t - \beta z) \quad (5-76) \\ \mathcal{H}_z &= \sqrt{2} H_0 \cos \frac{\pi}{a} x \cos(\omega t - \beta z)\end{aligned}$$

where $\lambda_c = 2a$, $E_0 = H_0 Z_{TE}$, and λ_g is defined in Eq. (5-70).

A sketch of the TE_{10} fields for a plus z -directed wave is shown in Fig. 5-18 for $t = 0$ and $t = T/4$. An end view of the electric and magnetic fields is also shown. Notice that the mode pattern moves a distance $\lambda_g/4$ in a quarter of a period. Thus the velocity is $\lambda_g/T = f\lambda_g$, which is exactly the phase velocity of the wave. Also note that E_y and H_x are maximum along the $x = a/2$ plane and their values are independent of y since $n = 0$. With $m = 1$, the field components exhibit one half sine wave variation in the x direction. In the propagation direction, of course, all the field components exhibit one complete sinusoidal variation per guide wavelength λ_g .

Since the skin depth is very small at microwave frequencies, practically all the conduction currents reside on the inner surfaces of the conducting walls. As explained in Sec. 2-3 [Eq. (2-42)], the surface current per unit length (K) is equal and normal to the tangential component of H at the conducting surfaces. For example, at the narrow walls, the conduction currents are in the $\pm y$ direction and $|K_y| = |H_z|$ at $x = 0$ and $x = a$. The H_x components at $y = 0$ and $y = b$ are related to conduction currents on the broad walls that are directed along the propagation direction. This longitudinal current $|K_z| = |H_x|$ is sometimes referred to as the *power current*. A sketch of the conduction currents for the TE_{10} mode is shown in Fig. 5-19.

Characteristic impedance in waveguide. In order to apply transmission-line theory to waveguides, one must be able to determine the phase constant (β) or guide wavelength (λ_g) as well as the characteristic impedance (Z_0) of the particular guide configuration. Equations (5-69) and (5-70) provide the required relationships for β and λ_g . Characteristic impedance is defined in Eq. (3-18) as V^+/I^+ , where V^+ is the voltage between the conductors and I^+ is the conduction current in the propagation direction for the traveling wave. For TEM lines, Z_0 is uniquely defined since the value of $V^+ = -\int \vec{E} \cdot d\vec{l}$ is independent of the integration path. In the waveguide case, V^+ is a function of the integration path and therefore many definitions of Z_0 are possible.

For rectangular waveguide in the TE_{10} mode, the electric field is maximum at $x = a/2$. From Eq. (5-76), its rms value is $E_y = E_0 \lambda_c / \lambda_g$. Integrating directly from $y = 0$ to $y = b$ yields the voltage across the centerline of the waveguide. Namely,

$$V_\epsilon = E_0 b \frac{\lambda_c}{\lambda_g} = H_0 Z_{TE} b \frac{\lambda_c}{\lambda_g} \quad (5-77)$$

However, this represents only *one* possible voltage value between the points $y = 0$, $x = a/2$ and $y = b$, $x = a/2$. For instance, one could integrate $\vec{E} \cdot d\vec{l}$ by choosing a path along the conducting walls. In this case $V_\epsilon = 0$. Other paths leading to different values of voltage are indicated in Fig. 5-29. Clearly, voltage and hence Z_0 does not have a unique value in waveguide. One possible definition is the ratio of V_ϵ as defined in Eq. (5-77) to the longitudinal current I_z , where

$$I_z = \int_0^a K_z dx = \int_0^a H_x dx$$

Integration along the bottom wall ($y = 0$) yields

$$I_z = H_0 \frac{\lambda_c}{\lambda_g} \int_0^a \sin \frac{\pi}{a} x dx = \frac{2a}{\pi} H_0 \frac{\lambda_c}{\lambda_g} \quad (5-78)$$

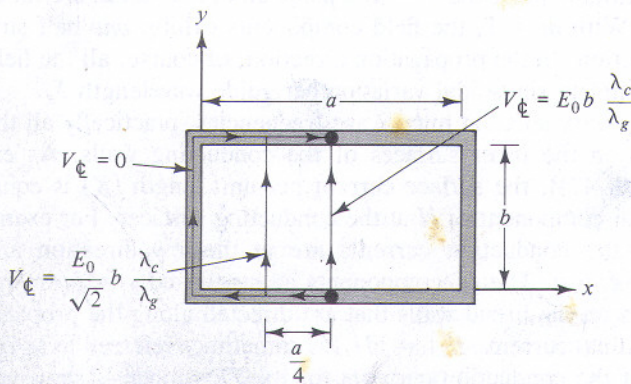


Figure 5-29 Possible integration paths for determining V_ϵ in rectangular guide.

where H_x , the rms value of \mathcal{H}_x , is obtained from Eq. (5-76). Therefore,

$$Z_0 = \frac{V_t}{I_z} = \frac{\pi b}{2 a} Z_{TE} = \frac{592 \frac{b}{a} \sqrt{\frac{\mu_R}{\epsilon_R}}}{\sqrt{1 - \left(\frac{f_c}{f}\right)^2}} \text{ ohms} \quad (5-79)$$

where Z_{TE} is given by Eq. (5-63). Since V_t and I_z are in phase, Z_0 is real for $f > f_c$. The above expression is known as the *voltage-current* definition of Z_0 . Other commonly used definitions are based upon power flow along the waveguide. These are

1. Power-Current Definition:

$$Z_0 = \frac{P}{I_z^2}$$

2. Power-Voltage Definition:

$$Z = \frac{V_t^2}{P}$$

3. Modified Power-Voltage Definition:

$$Z_0 = \frac{V_t^2}{P}$$

where V_t is given by Eq. (5-77) and I_z by Eq. (5-78). An expression for power flow in the z direction can be developed with the aid of Poynting's theorem [Eq. (2-58)]. With E_x and H_y in phase,

$$P = \int_S (\vec{E} \times \vec{H}) \cdot d\vec{S} = \int_0^a \int_0^b E_x H_y dy dx$$

and therefore

$$P = H_0^2 Z_{TE} \left(\frac{\lambda_c}{\lambda_g} \right)^2 b \int_0^a \sin^2 \frac{\pi}{a} x dx$$

or

$$P = \frac{1}{2} H_0^2 Z_{TE} ab \left(\frac{\lambda_c}{\lambda_g} \right)^2 \quad (5-80)$$

Applying this equation to the three definitions results in the following expressions for Z_0 in rectangular guide.

Power-Current Definition:

$$Z_0 = 465 \frac{b}{a} \sqrt{\frac{\mu_R}{\epsilon_R} \frac{\lambda_g}{\lambda}} \text{ ohms}$$

Power-Voltage Definition:

$$Z_0 = 754 \frac{b}{a} \sqrt{\frac{\mu_R}{\epsilon_R} \frac{\lambda_g}{\lambda}} \text{ ohms} \quad (5-81)$$

Modified Power-Voltage Definition:

$$Z_0 = 377 \frac{b}{a} \sqrt{\frac{\mu_R}{\epsilon_R} \frac{\lambda_g}{\lambda}} \text{ ohms}$$

where $\frac{\lambda_g}{\lambda} = \frac{1}{\sqrt{1 - (f_c/f)^2}}$.

given by

$$Z_{TM} = \frac{\beta}{\omega\epsilon} = \eta \sqrt{1 - \left(\frac{\lambda}{\lambda_c}\right)^2} \quad \text{ohms} \quad (5-85)$$

where λ_c is obtained from Eq. (5-67). Since $k_x = m\pi/a$ and $k_y = n\pi/b$, k_c may be obtained from Eq. (5-64). By substituting Eq. (5-82) into Eq. (5-84), the transverse field components of the TM modes for plus z-directed waves are obtained.

$$\begin{aligned} \mathbf{H}_x &= jE_0 \frac{\omega\epsilon}{k_c^2} \frac{n\pi}{b} e^{-j\beta z} \sin \frac{m\pi}{a} x \cos \frac{n\pi}{b} y \\ \mathbf{H}_y &= -jE_0 \frac{\omega\epsilon}{k_c^2} \frac{m\pi}{a} e^{-j\beta z} \cos \frac{m\pi}{a} x \sin \frac{n\pi}{b} y \\ \mathbf{E}_x &= \pm Z_{TM} \mathbf{H}_y \quad \text{and} \quad \mathbf{E}_y = \mp Z_{TM} \mathbf{H}_x \end{aligned} \quad (5-86)$$

where E_0 indicates the amplitude of the wave.

With $\beta^2 = \omega^2\mu\epsilon - k_c^2$, the expressions for β , λ_c , f_c , λ_g , v_p , v_g , and α are the same as for TE waves (namely, Eqs. 5-66, 5-67, 5-68, 5-70, 5-71, 5-74, and 5-75, respectively). Note that for a given set of values for m and n , the above expressions are the same whether the mode is TE or TM. For example, the cutoff frequency for the TE_{21} mode is the same as for the TM_{21} mode.

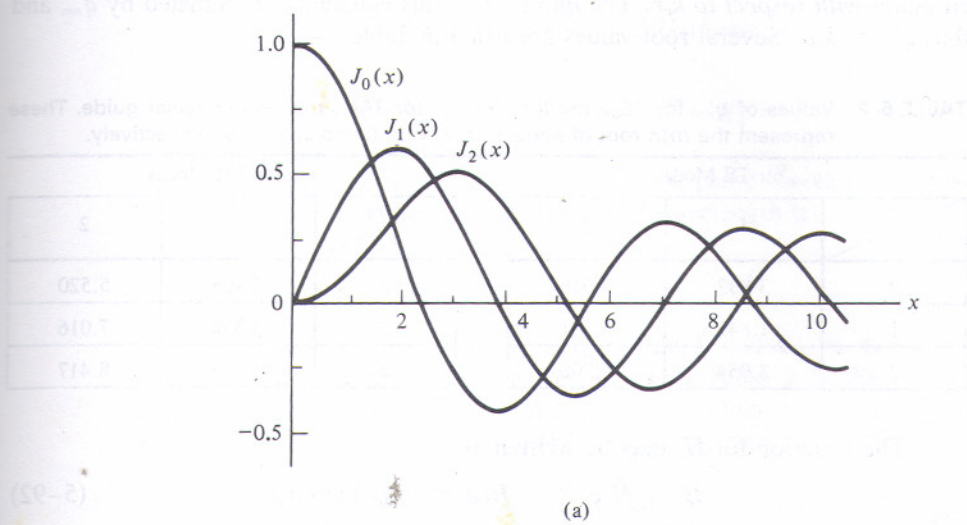
The TM mode with the lowest cutoff frequency in rectangular waveguide is the TM_{11} . For TM modes, the case where either $m = 0$ or $n = 0$ is trivial since all the field components reduce to zero. A sketch of the TM_{11} mode is shown in Fig. 5-20. It is obtained by converting Eqs. (5-82) and (5-86) into their time-varying form and letting $t = 0$. Viewed in the transverse plane, the TM_{11} mode looks similar to the TEM mode in stripline (Fig. 5-7). The only substantial difference is that the conduction current in the center conductor of the stripline is replaced by a displacement current. The existence of the E_z component in the waveguide results in the cutoff effect which, of course, does not occur in TEM lines. The cutoff wavelength for the TM_{11} mode is indicated in Fig. 5-20. By proper selection of waveguide height (b), this mode can be suppressed without affecting TE_{10} propagation. For $b = a/2$, the TM_{11} cutoff frequency is about 12 percent greater than that of the TE_{20} mode, and hence does not further restrict the usable frequency range of the waveguide.

5-5b Circular Waveguide Transmission

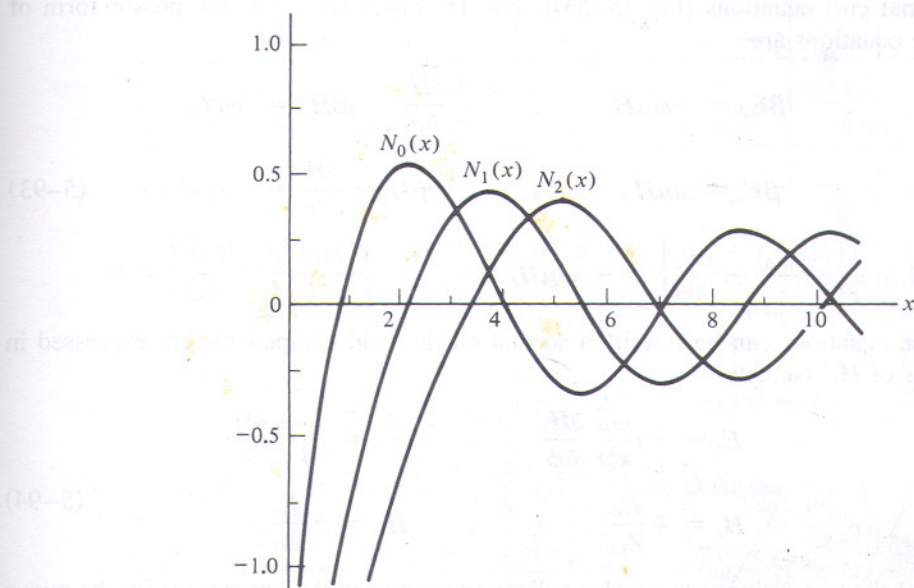
Figure 5-30 shows a circular waveguide of inner radius a . The coordinate system used in this discussion is also shown. A perfectly conducting guide wall and a uniform, loss-free dielectric region are assumed. The analysis that follows is similar to that for rectangular waveguide transmission.

In cylindrical coordinates, the z components of Eqs. (5-54) and (5-55) may be written as

$$\frac{1}{r} \frac{\partial}{\partial r} \left(r \frac{\partial \mathbf{E}_z}{\partial r} \right) + \frac{1}{r^2} \frac{\partial^2 \mathbf{E}_z}{\partial \phi^2} = -k_c^2 \mathbf{E}_z \quad (5-87)$$



(a)



(b)

Figure 5-31 Bessel functions of the first kind (part a) and of the second kind (part b).

$$\begin{aligned} \frac{1}{r} \frac{\partial E_z}{\partial \phi} + j\beta E_\phi &= -j\omega\mu H_r , \quad \beta H_\phi = \omega\epsilon E_r \\ j\beta E_r + \frac{\partial E_z}{\partial r} &= j\omega\mu H_\phi , \quad \beta H_r = -\omega\epsilon E_\phi \\ \frac{1}{r} \left\{ \frac{\partial(rE_\phi)}{\partial r} - \frac{\partial E_r}{\partial \phi} \right\} &= 0 , \quad \frac{1}{r} \left\{ \frac{\partial(rH_\phi)}{\partial r} - \frac{\partial H_r}{\partial \phi} \right\} = j\omega\epsilon E_z \end{aligned} \quad (5-103)$$

These equations can be rewritten so that all the field components are expressed in terms of E_z . Namely,

$$\begin{aligned} H_r &= j \frac{\omega\epsilon}{k_c^2 r} \frac{\partial E_z}{\partial \phi} , \quad H_\phi = -j \frac{\omega\epsilon}{k_c^2 r} \frac{\partial E_z}{\partial r} \\ E_r &= \pm Z_{TM} H_\phi , \quad E_\phi = \mp Z_{TM} H_r \end{aligned} \quad (5-104)$$

where the upper signs are for plus z -directed waves and the lower signs for minus z -directed waves. Z_{TM} , the wave impedance for TM waves, is given by

$$Z_{TM} = \frac{\beta}{\omega\epsilon} = \eta \sqrt{1 - \left(\frac{\lambda}{\lambda_c} \right)^2} \quad \text{ohms} \quad (5-105)$$

where $\lambda_c = K_{nm}D$. Values of K_{nm} for several TM modes are listed in Table 5-3. As before, the cutoff frequency can be determined from Eq. (5-68), while λ_g , v_p , v_g , and α are given by Eqs. (5-70), (5-71), (5-74), and (5-75), respectively.

The transverse field components for plus z -directed TM_{nm} modes are obtained by substituting Eq. (5-102) into Eq. (5-104). With some algebraic manipulation, the expressions can be written as

$$\begin{aligned} H_r &= -jH_0 n \frac{\lambda_c}{\lambda_g} \left(\frac{\lambda_c}{2\pi r} \right) e^{-j\beta z} J_n(k_c r) \sin n\phi \\ H_\phi &= -jH_0 \frac{\lambda_c}{\lambda_g} e^{-j\beta z} J'_n(k_c r) \cos n\phi \\ E_r &= Z_{TM} H_\phi \quad \text{and} \quad E_\phi = -Z_{TM} H_r \end{aligned} \quad (5-106)$$

where $H_0 = E_0/Z_{TM}$. The lowest-order TM mode in circular guide is the TM_{01} , which has a cutoff wavelength $\lambda_c = 1.306D$. Its transverse field pattern is shown in Fig. 5-27. Note that with $n = 0$, both H_r and E_ϕ are zero. The attenuation characteristic of the TM_{01} mode is shown in Fig. 5-28. An expression for α_c is derived in Sec. 8.04 of Ref. 5-6.

In concluding this section, it should be noted that Refs. 5-6 and 5-12 provide excellent mathematical treatments of electromagnetic transmission in waveguides and are recommended for further study.